Elastic Scattering of Protons by Nuclei*

D. M. CHASE AND F. ROHRLICH†
Palmer Physical Laboratory, Princeton University, Princeton, New Jersey
(Received December 9, 1953)

Exact calculations are carried out for the optical model in the 20-Mev region. A complex potential of spherical well shape is assumed in addition to the Coulomb potential. Results for the elastic scattering of protons by Al, Cu, and Ag are compared with experiments. Though all relevant parameters are varied over large domains, no satisfactory agreement is obtained. Various possible alternatives are discussed. It is also shown that the "boundary condition model" offers a good approximation to the optical model within its range of validity.

1. INTRODUCTION

THE optical model for the scattering of mesons and nucleons by nuclei has enjoyed considerable success. In this model the interaction of the incident particle with the individual constituents of the scattering nucleus is represented by an effective potential which enables one to reduce the problem to an equivalent one-body problem. The effective potential is in general complex, thus making a rather close analogy with the scattering of an electromagnetic wave by a medium of complex index of refraction.

The first success of the optical model was in high-energy neutron scattering.[1] Later, meson reactions were analyzed,[2] and, most recently, low-energy neutron scattering data were very successfully explained by this model.[3] Though the eventual theoretical justifications for the model may be of very different nature at high and low energies, respectively, it is reasonable to expect satisfactory results also at intermediate energies. Indeed, Le Levier and Saxon[4] obtained fairly good agreement with the elastic proton scattering experiments on Al at 18.6 Mev.[5] However, further experiments[6] soon showed that the calculated differential cross section is too large near 180° and in general too flat. For these reasons it was felt that further investigation of the 20-Mev region is appropriate.

Unfortunately, all recent experimental differential cross sections at that energy are for protons rather than for neutrons. Since the Coulomb and nuclear potentials are here of equal importance, this fact implies a considerable complication of the calculations. We have carried out exact calculations for several elements on the basis of the optical model but were limited by the lack of tables of Coulomb functions for parameters corresponding to proton scattering by elements of $Z>50$. Results are presented for Al, Cu, and Ag.

In addition to allowing a comparison with experiments, the exact calculations also enable one to check on approximate theoretical treatments. In particular, the boundary condition model is here investigated.[7] In this model it is assumed that the logarithmic derivative of the wave function ψ_l at the boundary R of the nucleus is independent of the angular momentum l of the incident particle, and that inside the nucleus ψ_l is of the form of an ingoing wave only:

$$u_l=r\psi_l\sim\exp(-ik'r). \tag{1}$$

k' is an average wave number of the incident particle inside the nucleus. This assumption is expected to be valid when the energy of incidence is sufficiently high so that exit through the entrance channel after penetration into the nucleus is very improbable. The logarithmic derivative at the boundary is

$$f_l=(d\ \ln u_l/d\ \ln r)_{r=R}=-ik'R. \tag{2}$$

This relation provides an approximate treatment of the optical model. The results of this treatment will be compared with those of the exact calculation.

In the next section we shall outline the method of calculation and in Sec. 3 we shall present the results for a variety of parameters. These are compared with the results of several experimenters and lead to the conclusions stated in the final section.

2. METHOD OF CALCULATION

A nonrelativistic particle in a complex potential satisfies in a stationary state the Schrödinger equation

$$\nabla^2\psi+(2M/\hbar^2)[E-V(r)-iW(r)]\psi=0, \tag{3}$$

where V and W are the real and imaginary part of the potential. In the usual way one finds an equation of continuity,

$$\partial\rho/\partial t+\nabla\cdot\mathbf{j}=(2\rho/\hbar)W, \tag{4}$$

* Supported in part by the U. S. Atomic Energy Commission and the Higgins Scientific Trust Fund.

† Now at the Department of Physics, State University of Iowa, Iowa City, Iowa.

[1] Fernbach, Serber, and Taylor, Phys. Rev. **75**, 1352 (1949).

[2] H. A. Bethe and R. R. Wilson, Phys. Rev. **83**, 690 (1951); Brueckner, Serber, and Watson, Phys. Rev. **84**, 258 (1951).

[3] Feshbach, Porter, and Weisskopf, Phys. Rev. **91**, 453 (1953); **90**, 166 (1953).

[4] R. E. Le Levier and D. S. Saxon, Phys. Rev. **87**, 40 (1952).

[5] J. W. Burkig and B. T. Wright, Phys. Rev. **82**, 451 (1951).

[6] P. C. Gugelot, Phys. Rev. **87**, 525 (1952), and unpublished work. I. E. Dayton (private communication). Dr. Dayton has kindly allowed us to quote some of his preliminary results. The qualitative features of his work are confirmed by relative cross section measurements at 21.5 Mev reported by B. L. Cohen and R. V. Neidigh, Phys. Rev. **93**, 282 (1954). We are grateful to Dr. Cohen for a prepublication copy of this paper.

[7] H. Feshbach and V. F. Weisskopf, Phys. Rev. **76**, 1550 (1949).

with $\rho=\psi^*\psi$ and $\mathbf{j}=(\hbar/2Mi)(\psi^*\nabla\psi-\psi\nabla\psi^*)$. It follows that the nucleus absorbs the incident beam of particles at a rate $(2\rho/\hbar)|W|$, $(W<0)$. We shall assume

$$V(r)=\begin{cases}-V_0 & (r<R)\\ Ze^2/r & (r>R)\end{cases},\quad W(r)=\begin{cases}-W_0 & (r<R)\\ 0 & (r>R)\end{cases}, \tag{5}$$

where R is the radius of the nucleus. The potential (5) corresponds to the assumption that the charge of the nucleus is distributed uniformly over its *surface*. If the nucleus had a uniform charge density throughout its *volume* a correction would have to be added for $r<R$ which is small compared to V_0. Also, the large absorption—the experimental absorption cross section is approximately geometrical—would prevent the incident particle from penetrating deep enough to detect such variations of the potential. The parameters Z, R, V_0, W_0 completely characterize the nucleus in this model.

The solutions u_l of the radial equation for each orbital angular momentum l are nonrelativistic Coulomb wave functions: $F_l(kr)$ and $G_l(kr)$ for $r>R$, and $k'rj_l(k'r)$ for $r<R$. Here,

$$k^2=2ME/\hbar^2,\quad k'^2=k^2+(2M/\hbar^2)(V_0+iW_0), \tag{6}$$

and j_l is the regular spherical Bessel function of order l. The phase shifts are obtained from the requirement of smoothness of the wave function. We define the logarithmic derivative at $r=R$ as in Eq. (2):

$$f_l=a_l+ib_l. \tag{7}$$

The calculation now proceeds in the usual way,[8] except that k'^2 is a complex number. Therefore, the solution u_l will also be complex and the phase shifts will be of the form

$$\delta_l+i\epsilon_l. \tag{8}$$

For the comparison of f_l on both sides of the discontinuity we find

$$f_l=\frac{k'Rj_l'(k'R)}{j_l(k'R)}+1=\frac{kR[F_l'(kR)+\tan(\delta_l+i\epsilon_l)G_l'(kR)]}{F_l(kR)+\tan(\delta_l+i\epsilon_l)G_l(kR)}. \tag{9}$$

An easy calculation yields from this:

$$\exp(-4\epsilon_l)=1-4r_l/[t_l^2+(r_l+1)^2], \tag{10}$$

$$\delta_l=-\arg(G_l+iF_l)+\tfrac{1}{2}\arg[t_l+i(r_l-1)]-\tfrac{1}{2}\arg[t_l+i(r_l+1)], \tag{11}$$

where

$$t_l=G_lG_l'+F_lF_l'-(F_l^2+G_l^2)a_l/kR, \tag{12}$$

$$r_l=(F_l^2+G_l^2)|b_l|/kR; \tag{13}$$

the differentiation is with respect to kr, and all functions are to be taken at $r=R$.

[8] See, e.g., J. M. Blatt and V. F. Weisskopf, *Theoretical Nuclear Physics* (John Wiley and Sons, Inc., New York, 1952).

In order to evaluate the phase shifts from Eqs. (10) and (11) the Coulomb functions must be known and the functions $j_l(k'R)$ and $j_l'(k'R)$ in Eq. (9) must be separated into their real and imaginary parts. For the determination of the Coulomb functions F_l and G_l the tables by Breit and collaborators proved most helpful.[9] However, four and five point interpolation and extrapolation is necessary in some cases, since the tables list only functions for angular momenta $l\leq 4$ and these must be known very accurately so that recursion formulas can be used to obtain functions for higher values of l. For a given argument $\rho=kR$ and parameter $\eta=Ze^2/\hbar v$ the four functions F_l, F_l', G_l, and G_l' are connected by the following relations:[10]

$$F_l'G_l-G_l'F_l=1, \tag{14}$$

$$F_{l-1}G_l-F_lG_{l-1}=l/[l^2+\eta^2]^{\frac{1}{2}}, \tag{15}$$

$$(l+1)[l^2+\eta^2]^{\frac{1}{2}}Y_{l-1}-(2l+1)(\eta+l(l+1)/\rho)Y_l+l[(l+1)^2+\eta^2]^{\frac{1}{2}}Y_{l+1}=0, \tag{16}$$

$$(l+1)Y_l'-((l+1)^2/\rho+\eta)Y_l+[(l+1)^2+\eta^2]^{\frac{1}{2}}Y_{l+1}=0, \tag{17}$$

$$lY_l'+(\eta+l^2/\rho)Y_l-[l^2+\eta^2]^{\frac{1}{2}}Y_{l-1}=0, \tag{18}$$

where

$$Y_l=G_l+iF_l.$$

These relations are not all independent. In particular, Eqs. (14) and (15) follow from (17) and (18). If, for a definite l, any three of the set of four values (F_l, F_l', G_l, G_l') are known, this set can be calculated for all values of l. For example, all F_l, F_l', G_l, G_l' can be calculated from F_0', F_0, and G_0. However, as one proceeds to larger l the accuracy decreases rapidly. In this connection those of relations (14) to (18) which seem superfluous can be used advantageously in checking the numerical work. Unfortunately, the range of the argument of the aforementioned tables is not sufficient for heavy elements at 20 Mev. Indeed, for 18.3 Mev and the usual nuclear radius [see Eq. (22)] one finds for Ag: $kR=6.36$, which is just outside the range of the tables but can be reached by extrapolation.

The separation of $j_l(k'R)$ into its real and imaginary part can be accomplished either by the series

$$j_l(x+itx)=(1+it)^l\sum_{n=0}^{\infty}j_{l+n}(x)(tx)^n(\tfrac{1}{2}t-i)^n/n!, \tag{19}$$

or by expressing j_l in terms of sine and cosine functions of complex argument. The separation j_l' can be reduced to that of j_l and j_{l-1} by well-known relations among Bessel functions. The spherical Bessel functions j_l of real argument are tabulated.[11]

[9] Bloch, Hull, Broyles, Bouricius, Freeman, and Breit, Revs. Modern Phys. **23**, 147 (1953).

[10] J. L. Powell, Phys. Rev. **72**, 626 (1947).

[11] National Bureau of Standards, Mathematical Tables Project, *Tables of Spherical Bessel Functions* (Columbia University Press, New York, 1947).

After these somewhat laborious auxiliary calculations the phase shifts can be obtained from Eqs. (10) and (11). The differential cross section is found to be

$$d\sigma/d\Omega=(S^2+T^2)/4k^2, \tag{20a}$$

$$S(\vartheta)=\sum_{l=0}^{\infty}(2l+1)[\exp(-2\epsilon_l)\cos(2\delta_l+2\sigma_l) -\cos 2\sigma_l]P_l(\cos\vartheta)+(\eta/\sin^2\tfrac{1}{2}\vartheta) \times\sin(2\sigma_0-2\eta\ln\sin\tfrac{1}{2}\vartheta), \tag{20b}$$

$$T(\vartheta)=\sum_{l=0}^{\infty}(2l+1)[\exp(-2\epsilon_l)\sin(2\delta_l+2\sigma_l) -\sin 2\sigma_l]P_l(\cos\vartheta)-(\eta/\sin^2\tfrac{1}{2}\vartheta) \times\cos(2\sigma_0-2\eta\ln\sin\tfrac{1}{2}\vartheta). \tag{20c}$$

The Coulomb phase shifts σ_0 can also be found in tables.[12]

The absorption cross section is

$$\sigma_a=(\pi/k^2)\sum_{l=0}^{\infty}(2l+1)[1-\exp(-4\epsilon_l)]. \tag{21}$$

It is not explicitly dependent on the Coulomb potential. The formulas (20) express clearly the coherent effect of the Coulomb and nuclear scattering. It is clear from these equations that the amplitudes cannot be written as the sum of an exclusively Coulomb and another, exclusively nuclear, contribution. This fact makes the strict concept of interference between two scattering effects inapplicable for the case of Coulomb and nuclear scattering. Nevertheless, we shall refer to such interference in the sense of comparison of this scattering with pure Coulomb scattering. For simplicity we shall take the pure Coulomb scattering for a point nucleus (Rutherford scattering).

The summation in the first term of $S(\vartheta)$ and $T(\vartheta)$ in (20) extends up to the highest angular momentum l_1 which contributes to the nuclear scattering. For Al, l_1 is about 5 or 6, whereas for Ag, $l_1=7$.

3. RESULTS[13]

We choose for the nuclear radius

$$R=1.42A^{\frac{1}{3}}\times10^{-13}\text{ cm}, \tag{22}$$

and for the energy 18.3 Mev, the energy at which Gugelot's experiments are carried out. The results are not very sensitive to the choice of R as will be shown below. The choice of V_0 and W_0 is somewhat arbitrary. A reasonable value would perhaps be $V_0=30$ Mev, corresponding to the usual Fermi gas well, where for light elements (Al) one may expect that the Coulomb barrier of a few Mev should be subtracted; Le Levier and Saxon claim best results with $V_0=45$ Mev. The value of W_0 for a given V_0 depends, of course, on the energy. The optical model gives the relation

$$W_0=2[V_2(E+V_0)+V_2^2]^{\frac{1}{2}}, \tag{23}$$

where $V_2=\hbar k_2^2/2M$, $k_2=\mathrm{Im}k'$. We can introduce the penetration depth Λ which is the distance a nucleon beam travels in nuclear matter before its intensity is reduced by $1/e$. It follows that $2\Lambda=1/k_2$. For practical purposes V_2 can be neglected compared to $E+V_0$ such that Eq. (23) may be written conveniently

$$W_0=4.5(E+V_0)^{\frac{1}{2}}/\Lambda, \tag{24}$$

where the energies are in Mev and Λ is in units of 10^{-13} cm. We can obtain an estimate of W_0 at 20 Mev by a somewhat daring extrapolation from the 90-Mev neutron data. The penetration depth Λ may be taken approximately equal to the mean free path in nuclear matter. The latter increases at most proportionally to $E+V_0$, but at lower energies the exclusion principle will reduce this dependence considerably. With these assumptions we find from[1] $\Lambda(90\text{ Mev})\sim4\times10^{-13}$ cm, $V_0\sim30$ Mev, a value $\Lambda(20\text{ Mev})\sim1.7\times10^{-13}$ cm. Equation (24) now gives $W_0\sim20$ Mev. The potential $-V=30+20i$ Mev thus seems to be a reasonable first approximation near $E=20$ Mev.

The most important results of our calculations are shown in Figs. 1 to 6, together with experimental

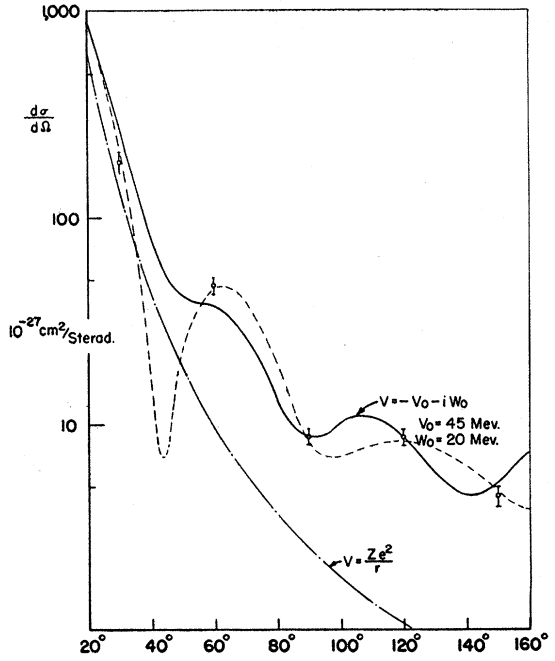

FIG. 1. Elastic scattering of protons by aluminum. The solid curve is the result of an exact calculation at 18.3 Mev. The dashed curve represents the experimental results of Dayton at 19.1±0.2 Mev. The experimental points in this and the following figures are those of Gugelot at 18.3 Mev.

[12] See, for example: National Bureau of Standards, *Tables of Coulomb Functions* (U. S. Government Printing Office, Washington, D. C., 1952), Vol. 1.

[13] Most of the results discussed in this section were first reported at the Washington Meeting of the American Physical Society, May, 1953; see F. Rohrlich and D. M. Chase, Phys. Rev. **91**, 454 (1953).

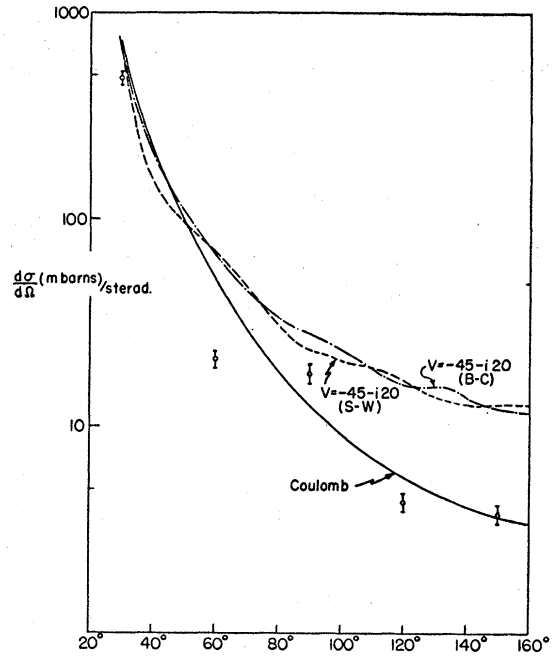

FIG. 2. 18.3-Mev protons on Cu. The good approximation offered by the boundary condition model is compared with the exact calculation (square well shape).

results of Gugelot and of Dayton.[6] These are the only experiments at the present time which give absolute values of the cross section.

In Fig. 1 we present the recalculated Al cross section for $-V=45+20i$ Mev first obtained by Le Levier and Saxon.[4] The calculations agree with the general trend of the measured differential cross section but certainly do not reproduce the pronounced maxima and minima. We notice that nuclear and Coulomb scattering interfere constructively for Al in the sense that the measured cross section over most of the angular range is greater than that for pure Coulomb scattering from a point nucleus.

On the other hand, there is no constructive interference for Cu (Fig. 2). The experimental points indicate that the total scattering cross section is about equal to that for Coulomb scattering. The two theoretical curves for $-V=45+20i$ Mev represent the exact optical model and the boundary-condition model, respectively.

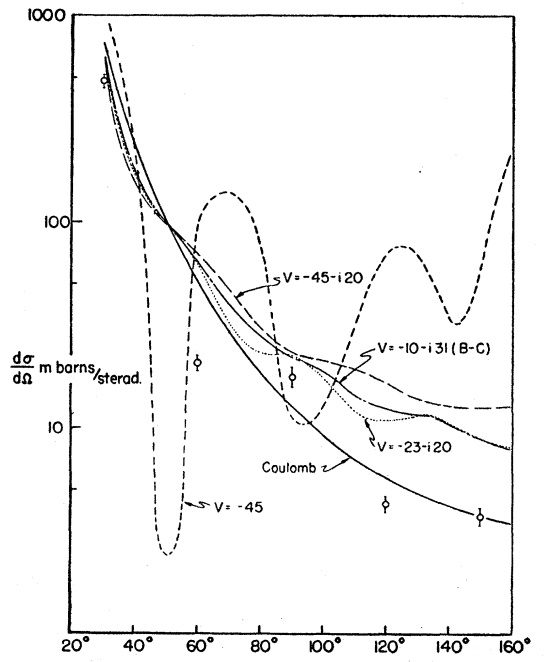

FIG. 3. 18.3-Mev protons on Cu. The dependence of the cross section on V_0 and W_0 is exhibited.

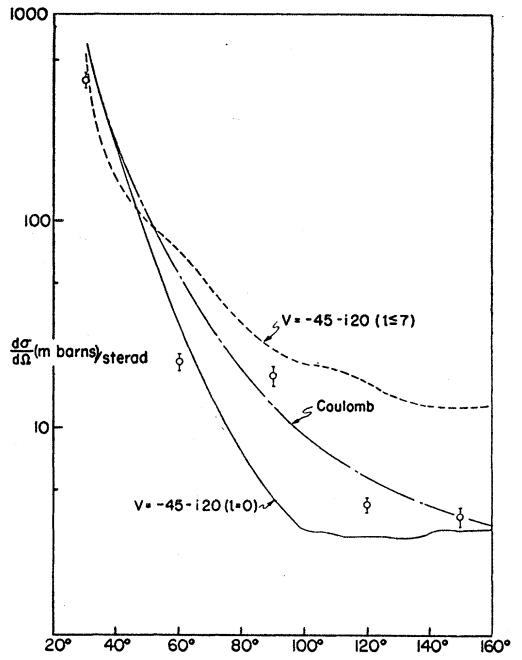

FIG. 4. 18.3-Mev protons on Cu. At large angles the cross section is about four times s-wave scattering in a Coulomb field.

The latter is seen to give a fairly good approximation to the former, but is in general smoother, i.e., it shows less pronounced minima and maxima. Both curves are far above the experimental data.

In order to study the dependence of the theoretical cross section on V_0 and W_0, in Fig. 3 several extreme assumptions are compared with the results of Fig. 2. The effect of a relatively too small absorptive part, W_0, is seen in the extreme case, $-V=45$ Mev. The angular variations are much too large and the cross section is orders of magnitude too large for angles above 90°. (This result is of special interest in connection with the potential $-V=20+i$ Mev recently proposed by Weisskopf[3] which explains the total neutron cross sections below 3 Mev.) However, a reduction of the real part

of V by a factor of two or even four has relatively little effect as long as the imaginary part is kept large.

One might be inclined to think that for large angles the scattering is primarily due to s waves. That this is not at all the case is shown in Fig. 4, where s scattering is compared with previous results. Indeed, s scattering accounts for only one-fourth of the cross section at large angles. (The Coulomb scattering is, of course, always *fully* taken into account.)

For larger Z, nuclear and Coulomb scattering interfere destructively (in the above sense). The actual cross section is only a fraction of Coulomb scattering. Figure 5 shows the results for Ag. A reasonable potential, $-V=35+20i$ Mev, gives about six times more scattering than is observed. Even a rather extreme case, $-V=5+5i$ Mev, gives much too much scattering between 70° and 150°.

Finally, in Fig. 6 we show the effect of a variation of the nuclear force range. Conveniently, only the first five phase shifts were calculated. For Cu, $kR=5.33$ if we use Eq. (22). The corresponding cross section (in the boundary condition approximation for $-V=45+20i$ Mev) is shown, first with all contributing partial waves ($l\leq 7$) included, and again with only the first five included. Also shown are the cross sections for two different radii corresponding to $kR=5.0$ and 5.8 ($l\leq 4$). We see that even a variation of almost ±10 percent leaves the theoretical curves several times higher than the measured values.

A number of further results will be mentioned in the following section.

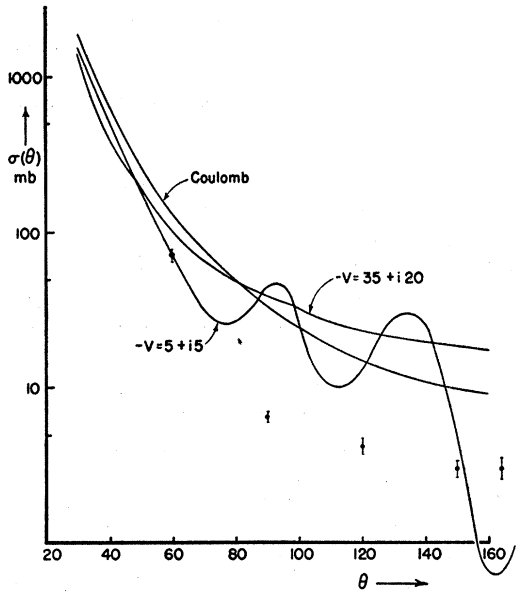

FIG. 5. 18.3-Mev protons on Ag.

4. CONCLUSIONS AND DISCUSSION

(1) Comparison of the differential cross section in the approximation of the boundary-condition model with that from exact calculations shows that this approximation yields very good results, but gives somewhat less pronounced structure. A typical instance is shown in Fig. 2.

(2) When the experimental results are compared with pure Coulomb scattering by a point nucleus, a marked dependence on Z appears: For small Z the nuclear forces contribute constructively to the scattering; for $Z\sim 29$ (Cu) they do not change the total scattering cross section, but cause maxima and minima in the differential cross section; for larger Z they contribute destructively. This Z dependence is most pronounced at large angles, as can be seen from the following four cases at 150°:

Z	13	29	47	78
$\sigma_{\text{exp}}(150°)/\sigma_{\text{Coul}}(150°)$	6.1	1.0	0.31	0.16

(3) The optical model with a square well shape and with the accepted nuclear radii [Eq. (22)] gives considerably more scattering than an equally large point charge, so that reasonable agreement with experiments can be attained only for small Z. This result is valid over a very large range of both V_0 and W_0 and over considerable variations of the nuclear range.

(4) The absorption cross section is found to be between 60 and 90 percent of the geometric cross section for $W_0\sim 20$ Mev in qualitative agreement with experiments.

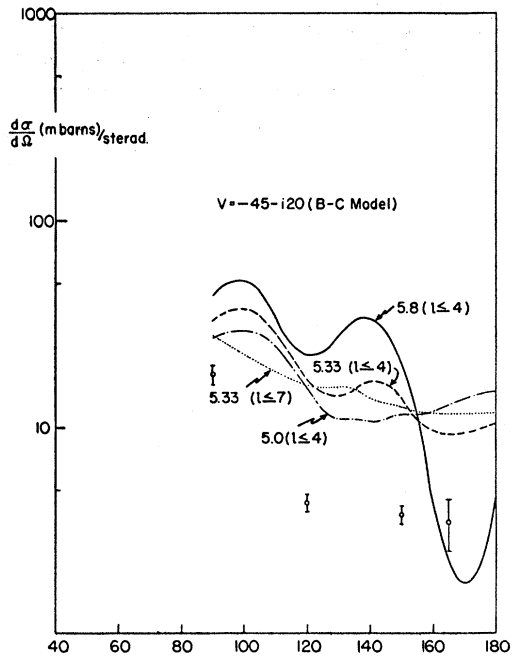

FIG. 6. 18.3-Mev protons on Cu, dependence of the cross section on the nuclear radius. The accepted radius ($kR=5.33$) gives an approximate cross section ($l\leq 4$) which is compared with cross sections for larger and smaller radii in the same approximation.

(5) The experimental minima and maxima of the differential cross section are more pronounced than can be reproduced by this optical model, if the absorption is to be large enough and the backward scattering small enough.

Several assumptions made in this paper can be held responsible for the negative results presented above. The lack of a "tail" of the nuclear potential and the consequent discontinuity of the total potential on the nuclear boundary is perhaps the most obvious defect of the model investigated here. Also, for wavelengths of 10^{-13} cm the assumption of a sharp nuclear boundary is questionable.

Other deficiencies include the neglect of the Pauli principle and the absence of other forces not usually included in the optical model. It should be pointed out that the large absorption does not permit a particle to be scattered after it has penetrated an appreciable distance into the nucleus. Therefore, the scattering cross section should be practically independent of the detailed shape of the potential for $r<R$. Furthermore, the experiments show no dependence on magic numbers or spins of the target nuclei. Spin-dependent forces, therefore, should not be of importance.

However, there seem to be at least two strong arguments in favor of a small absorption potential W_0. One is the excellent agreement of the potential[3] $-V=19(1+0.05i)$ Mev with the neutron scattering data up to 3 Mev; the other is the strong angular dependence of the 20-Mev proton scattering data observed by Cohen and Neidigh[6] and by Dayton (see Fig. 1). The steep maxima and minima require a very small W_0, perhaps of the order of 5 Mev. From Eq. (24) we see that this implies $\Lambda(20\text{ Mev})\sim 6.5\times 10^{-13}$ cm, which is of the order of magnitude of the radii of the investigated nuclei and means that the scattering would be much more sensitive to the shape of the potential well. In this case, it also follows that the extrapolation from the 90-Mev data with the accepted energy dependence of the mean free path [see the argument following Eq. (24)] is completely wrong and that Λ is actually a *decreasing* function of energy, at least for $E\lesssim 50$ Mev. This situation is in very nice agreement with the great success of the shell model at very low energies: the more independently the particles move, the larger is their mean free path. If we accept these arguments and use a potential $-V=30+20i$ Mev, say, then our calculations show that it may indeed be possible to fit the observed angular distribution for not too large angles (up to 90°, say), but that for larger angles this potential gives much too much scattering. The latter effect may then be blamed on the spherical well shape whose large discontinuity causes too much reflection. Thus, with these arguments we are led to believe that a potential of approximate magnitude $-V=30+5i$ Mev *which has a sufficiently long tail* may fit the observed angular distributions. However, such a model would probably give a rather small absorption cross section. Calculations along these lines are in progress.

It will be extremely interesting to study the scattering of neutrons by nuclei in this energy region. If the model presented here can account for neutron scattering, our results show that the optical model can give the correct nuclear scattering amplitude except for a phase factor. This phase factor is of no interest for neutron scattering, but is essential for proton scattering.

In conclusion, we wish to thank Professor P. C. Gugelot and Dr. I. E. Dayton for discussing their experimental results with us and Mrs. Ruth Shoemaker for her able help in the early stages of the numerical work.